ELSEVIER

Contents lists available at ScienceDirect

# Agriculture, Ecosystems and Environment

journal homepage: www.elsevier.com/locate/agee





# Water and nitrate loss from dryland agricultural soils is controlled by management, soils, and weather

W. Adam Sigler <sup>a,b,\*</sup>, Stephanie A. Ewing <sup>a</sup>, Clain A. Jones <sup>a,b</sup>, Robert A. Payn <sup>a,c</sup>, Perry Miller <sup>a</sup>, Marco Maneta <sup>d</sup>

- a Land Resources & Environmental Sciences, Montana State University, Bozeman, MT, United States
- <sup>b</sup> Montana State University Extension, Bozeman, MT, United States
- <sup>c</sup> Montana Institute on Ecosystems, Montana University System, MT, United States
- <sup>d</sup> Geosciences Department, University of Montana, Missoula, MT, United States

#### ARTICLE INFO

# Keywords: Soil moisture Deep percolation Leach Hydrus Rainfed

#### ABSTRACT

The vast majority (82 %) of the earth's cultivated area is not irrigated, and half is in semi-arid regions where water tends to limit crop growth. In dryland semi-arid agroecosystems, any precipitation not transpired indicates crop yield that is below potential. Precipitation that is partitioned to deep percolation can transport nitrate out of the root zone, reducing nitrogen use efficiency and potentially contaminating groundwater. To mitigate loss of crop yield to drought, the practice of chemical summer-fallow (suppressing plant growth for a full growing season with herbicide) has been common in semi-arid regions to store water for the following growing season. However, precipitation losses during fallow tend to exceed the amount of precipitation stored, and fallow tends to increase nitrate leaching. We present model simulations informed by field observations that explore the interaction of crop rotation, weather, and soils as controls on precipitation partitioning and nitrate leaching. Simulations reveal that high intensity precipitation periods produce hot moments of deep percolation and nitrate leaching such that 54 % of deep percolation and 56 % of leaching occurs in two of 14 model years. Simulations indicate that thin soils (having limited water storage capacity) produce hot spots for deep percolation and nitrate leaching such that thinner soils (<25 cm) experience water and nitrate loss rates five to 16 times higher than thicker soils (>100 cm). The practice of fallow facilitates mineralization of soil organic nitrogen to nitrate and increases deep percolation, magnifying the interaction of hot moments and hot spots. Simulations suggest that a field with fallow in rotation once every three years experiences 55 % of its deep percolation and 43 % of its leaching losses during fallow years.

## 1. Introduction

Fifteen million square kilometers of the earth's surface is cultivated (Ramankutty et al., 2008). Of that cultivated area, 82 % is not irrigated (Siebert et al., 2005), and approximately 50 % is in semi-arid regions (Ramankutty et al., 2008; Safriel and Adeel, 2005). Definitions vary, but the climate is generally considered semi-arid where annual precipitation is approximately 20–50% of potential evapotranspiration, and the regions classified as semi-arid are expanding with global-scale changes in climate (Huang et al., 2016). Without irrigation (dryland), crops grown on cultivated lands in semi-arid areas tend to be water limited, meaning that partitioning of precipitation to evaporation, overland flow, and percolation below the root zone can result in crop yields below potential

(Rockstrom and Falkenmark, 2000). This yield gap between actual and potential crop production is a loss of economic opportunity and more generally inhibits the ability to meet the challenges of feeding a growing human population (Cassman et al., 2003; Nielsen et al., 2005; Foley et al., 2011). Deep percolation may also transport nutrients out of the root zone, simultaneously reducing nitrogen (N) use efficiency and potentially degrading downgradient water quality (Spalding and Exner, 1993; Goulding, 2000; Di and Cameron, 2002; Smith, 2003; Tesoriero et al., 2013; Sigler et al., 2018). Cropping system management can influence efficient use of both water and N in food production, by regulating water storage and movement in soil. Thus, improved understanding of the interactions of dryland cropping systems with water and solute dynamics in soils is required to achieve reliable crop

E-mail address: asigler@montana.edu (W.A. Sigler).

 $<sup>^{\</sup>ast}$  Corresponding author.

yields and protection of water resources.

In semi-arid agricultural regions like the northern Great Plains of North America, chemical summer-fallow (fallow) is a common rotational practice of using herbicide to suppress plant growth over a full growing season to encourage water storage in the soil for crops grown during the subsequent year. Fallow practices strongly influence the partitioning of water and N in soils. Water stored in the rooting zone during fallow periods can mitigate risk of poor yields due to drought during the following season (Nielsen et al., 2002, 2005; Lawrence et al., 2018). However, extended periods of higher soil water content during fallow may also promote in-soil formation if nitrate with decomposition of soil organic matter, creating conditions primed for loss of both water and nitrate from the root zone (John et al., 2017). The benefit to yield resulting from water storage during fallow is quantified as the fraction of stored precipitation available for use by the subsequent crop (precipitation storage efficiency; PSE). Since the adoption of no-till and crop-residue management practices starting in the 1970s, the maximum PSE value observed in the Great Plains region has been ca. 40 %, but PSE is commonly less than 20 % (Peterson et al., 1996; Farahani et al., 1998; Nielsen et al., 2005). In addition to increasing subsequent yields, enhanced soil water content during fallow periods facilitates ammonification of soil organic N rapidly followed by nitrification of ammonium to nitrate, which we collectively term mineralization. Mineralization provides an added N supply available to the following year's crop, but mineralized nitrate may also be lost to leaching when subsequent precipitation exceeds the field capacity of the soil. In our study area of dryland wheat production in central Montana, Sigler et al. (2018) found evidence that fallow strongly influenced nitrate leaching rates estimated to be 11–18 kg N ha<sup>-1</sup> yr<sup>-1</sup> for a 260-km<sup>2</sup> terrace landform. In a companion study examining soil mass balance, John et al. (2017) found higher nitrate leaching (nitrate-N loss) rates at the field scale (ca. 80 acres or 0.32  $\rm km^2)$  post-fallow in a fallow-wheat sequence (54 kg N  $\rm ha^{-1}$  $yr^{-1}$ ) than post-pea in a pea-wheat sequence (18 kg N ha<sup>-1</sup>  $yr^{-1}$ ). Similarly, in another study of crop management in semi-arid systems, Campbell et al. (2006) found higher nitrate leaching rates over a 37-yr period with a wheat-fallow rotation (ca. 5 kg N ha $^{-1}$  yr $^{-1}$ ) than with a continuous cropping rotation (ca. 0 kg N ha $^{-1}$  yr $^{-1}$ ). Characterizing the connections between fallow practices and nitrate leaching in dryland systems requires holistic understanding of the coupling of soil water and N dynamics. This understanding in turn can inform land management decisions that influence the efficiency of water and nutrient use by crops in dryland agriculture.

Research on N dynamics and plant use efficiency in agricultural soils has been extensive, but we are aware of few studies that have integrated variation in crop rotation, soil properties, and weather to identify the particular times and places where water and N are not being used efficiently. Field trials have been conducted for decades to explore the effects of fallow on precipitation use efficiency in the Great Plains region (Farahani et al., 1998; Anderson et al., 1999; Nielsen and Vigil, 2017), and to a lesser degree, field trials have investigated the effects of fallow on nitrate leaching (Campbell et al., 2006; John et al., 2017). The few related studies that have used modeling approaches have focused on predicting yield and water use for various crop rotations (Anapalli et al., 2005; Saseendran et al., 2010). Modeling work has yet to address interactions of crop rotation, weather, and soils as controls on precipitation partitioning and nitrate leaching in the context of water quality implications. This gap in the literature underscores our limited understanding of the vulnerability of these agroecosystems to the increasing pressure for intensified agricultural production in a changing climate (Cassman et al., 2003; Lanning et al., 2010; Siebert et al., 2010).

Our objective in this work was to employ a hydrologic model informed by field data to explore how changes in evapotranspiration (ET) due to fallow practices interact with variable soil depths and weather patterns to control nitrate leaching via episodic deep percolation. Soils were characterized by combining soil pit observations with aerial imagery and SSURGO data. A one-dimensional soil water model

based on Richard's equation (Hydrus-1D v4.16; Simunek et al., 2013; Šimůnek et al., 2020) was used to characterize precipitation partitioning and nitrate leaching across a combination of crop rotation and soil water holding capacity scenarios for a 14-yr period in the Judith River Watershed, central Montana (Fig. 1). Results from this deep percolation modeling based approach were compared to previous estimates of nitrate leaching from companion studies, which estimated leaching rates based on N mass balance at the field scale (John et al., 2017) and water plus nitrate flux at the landscape scale (Sigler et al., 2018). We hypothesize that the reduction of ET by fallow practices increases soil water storage and mineralization of soil organic N. While these stored resources can benefit the subsequent crop, they also hydrologically prime soils for higher rates of deep percolation and biogeochemically prime soils for nitrate leaching in response to springtime precipitation the following year. More generally, we suggest that long-term use of fallow rotations is effectively a manipulative experiment that has created a shifting mosaic (Bormann and Likens, 1979) within dryland agroecosystems, where the larger-scale water and N budgets of the landscape emerge from an interaction of "hot spots" defined by areas with shallow soils and "hot moments" defined by periods of rain on soils primed for water and nitrate loss (McClain et al., 2003). We therefore hypothesize that the overlap of these key locations and key events for water and N transport has created predictable ecological control points (Bernhardt et al., 2017) that are the primary determinants of N use inefficiency of the agroecosystem as a whole.

#### 2. Methods

#### 2.1. Study area and cropping practices

The study area (Fig. 1) is located within the Judith River Watershed (HUC 10040103), which drains 7200 km² of central Montana into the Missouri River. Near the center of the study area, mean annual precipitation at the Montana State University Central Agricultural Research Center (CARC) is 39 cm (1909–2016 period of record at Western Regional Climate Center Station: WRCC 245761), with 37 % of mean annual precipitation occurring in May and June (Fig. 2). Precipitation measured during non-freezing months at fields selected for this study ranged from 50 to 140 % of the values reported for the WRCC gage at CARC between 2012 and 2014 (Sup Fig. 2.1a). Mean annual reference potential evapotranspiration (rPET) at CARC is 144 cm (2001–2016 at Agrimet Station: MWSM), resulting in an average precipitation to rPET ratio of 0.26 during the 15-yr period of the Agrimet record.

Nitrate-N concentrations in shallow aquifers recharged by infiltration through farmlands in the watershed are commonly above 20 mg L $^{-1}$  (U.S. EPA drinking water standard: 10 mg L $^{-1}$ ; Ward et al., 2005), and trends suggest concentrations approximately doubled from 1994 to 2011 (Sigler et al., 2018; Schmidt and Mulder, 2010). These relatively high nitrate concentrations have been associated with the common practice of summer-fallow, precipitation patterns, and soil characteristics (Bauder et al., 1993). Most soils overlying shallow aquifers in the area have relatively thin (ca. 30–100 cm) fine-textured horizons (typically clay loams) overlying relatively coarse subsurface horizons (>40 % gravel/cobble), resulting in modest water holding capacity and thus enhancing vulnerability of underlying shallow aquifers to contamination from inefficient fertilizer use.

Crops grown in the region are typically small grains including winter wheat (*Triticum aestivum* L.), spring wheat, and barley (*Hordeum vulgare* L.) with a year of fallow included in rotation every two to four years (Sigler et al., 2018). Fertilizer application rates associated with crop production are on the order of  $60-100~\rm kg~N~ha^{-1}~yr^{-1}$  (John et al., 2017). Irrigation is not common in the area, so production tends to be water-limited, and variation in yields tend to vary with the distribution of precipitation and its storage in soils.

Three study fields (Field A near Stanford, MT; Field B near Moccasin, MT; Field C near Moore, MT; Fig. 1) with similar soils were selected from

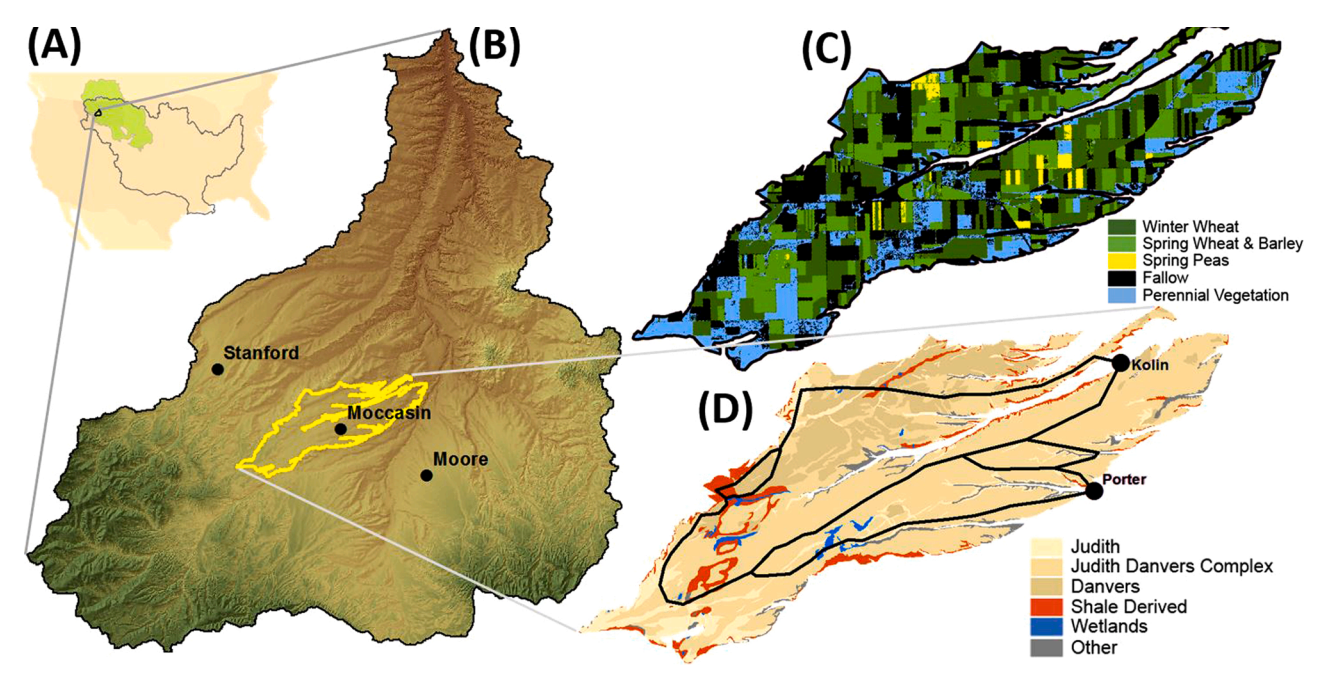


Fig. 1. Study area. (A) the location of the Judith River Watershed (JRW) study area within the northern Great Plains (green) and the Mississippi Atchafalaya River Basin (gray outline); (B) the locations of the Moccasin terrace and towns nearest to the study fields within the JRW; (C) land use on the Moccasin terrace in 2014; and (D) soils and sample sites for catchments (outlined with black lines) on the Moccasin terrace. (For interpretation of the references to colour in this figure legend, the reader is referred to the web version of this article).

areas managed by collaborating farmers on three different depositional landforms in the study area (Fig. 1: detailed field and management descriptions in John et al., 2017). Two crop rotations are addressed in this modeling work, based on practices currently employed in wheat production in the region. The 3-yr rotations include winter wheat, followed by spring grain, followed by either fallow ("with-fallow") or a second spring grain ("without-fallow"). Within each rotation are three possible rotational sequences, each offset by one year for a total of 6 rotational sequences (Fig. 3) that represent every combination of annual weather and crop or fallow. Crop years are delineated starting 1 April, reflecting approximate timing of winter wheat emergence in the area (Agrimet; start date for winter wheat crop coefficients), as well as initiation of spring grain seeding. We present results in the context of each 2-yr crop sequence within each rotation, designated by the field use in consecutive years (e.g., Fallow-Crop, Crop-Crop, Crop-Fallow), where the underlined descriptor indicates land use during the crop year of analysis and the prefix indicates land use during the previous crop year (Fig. 3).

The without-fallow rotation simulated in this work represents a continuous small grain rotation, which is not generally recommended due to pest control issues. However, the simulation of spring grain in place of fallow is expected to represent roughly similar hydrologic behavior as other fallow alternatives such as pulse crops (e.g., pea, lentil, chickpea). Research suggests that pulse crops may provide more sustainable diversification of crop rotations in at least some areas of Montana (Burgess et al., 2012; Miller et al., 2015).

# 2.2. Spatial distribution of soil thickness $(z_f)$

We characterized the spatial distribution of soil architecture using a combination of soil maps, direct observation from soil pits, and aerial imagery. The pertinent soil series from the SSURGO database (USDAb) have well drained, fine-textured clay loam surface horizons, underlain by coarser textured gravely loam horizons (Sup Section 2.2). For these soil series and for our own soil pits, we define the thickness of fine-textured soil ( $z_f$ ) as the depth at which the fine-textured horizons transition to coarser textured subsurface horizons with more than 40 % rock. More than seventy soil pits were excavated and described within the

three study fields between 2012 and 2013. Field C soils were further characterized using an aerial image from 24 July 2011 (USDAc), which depicts variable greenness across the field in a barley crop. Variation in greenness was hypothesized to be correlated with water availability as a function of  $z_f$ . Soil pits were dug at 19 locations within Field C (Fig. 1) during fallow in 2012. The  $z_f$  values observed from these pits were plotted versus a normalized difference vegetation index (NDVI) value calculated from the NAIP image for a 2-m buffer area around each soil pit. This relation was used to estimate the spatial distribution of  $z_f$  based on a 1-m resolution NDVI raster. The frequency distribution of  $z_f$  observed in soil pits and inferred from NDVI for Field C was used to characterize an example spatial distribution of  $z_f$  to estimate field-scale deep percolation and nitrate leaching.

Model results from this study were scaled using soil distribution data, allowing comparisons to previous landscape-scale characterizations of deep percolation and nitrate leaching rates for two catchments in the study area (Sigler et al., 2018; Fig. 1D). The scaling strategy applied inferred spatial distributions of  $z_f$  values from SSURGO soil series mapped in the catchments, as well as extensive observations from soil pits excavated as part of this study. Soils information from SSURGO data compiled by Sigler et al. (2018) indicates both catchments are dominantly (>80 %) comprised of Judith and Danvers soil series. Mean  $z_f$  values for the two series were characterized based on soil series descriptions (USDAa). For the purposes of a parsimonious scaling strategy, mean  $z_f$  for the Judith series was assumed to be 61 cm, corresponding to the mean depth to the gravel horizon (2Bk3) and mean  $z_f$  for the Danvers series was assumed to be 112 cm, corresponding to the minimum depth to the 2C horizon (Sup Table 2.2a).

## 2.3. Measuring nitrate in soil

Soils were sampled from 36 pits excavated in Fields B and C in 2012 and 2013. Of these 36 pits, 24 were excavated and sampled in July-August during fallow years (fallow since harvest approximately one year prior), and 12 were excavated and sampled in August-September following harvest (four in winter wheat and eight in barley). Soil volumes (1500 cm $^3$ ) were sampled at 15-cm depth increments along 10  $\times$ 

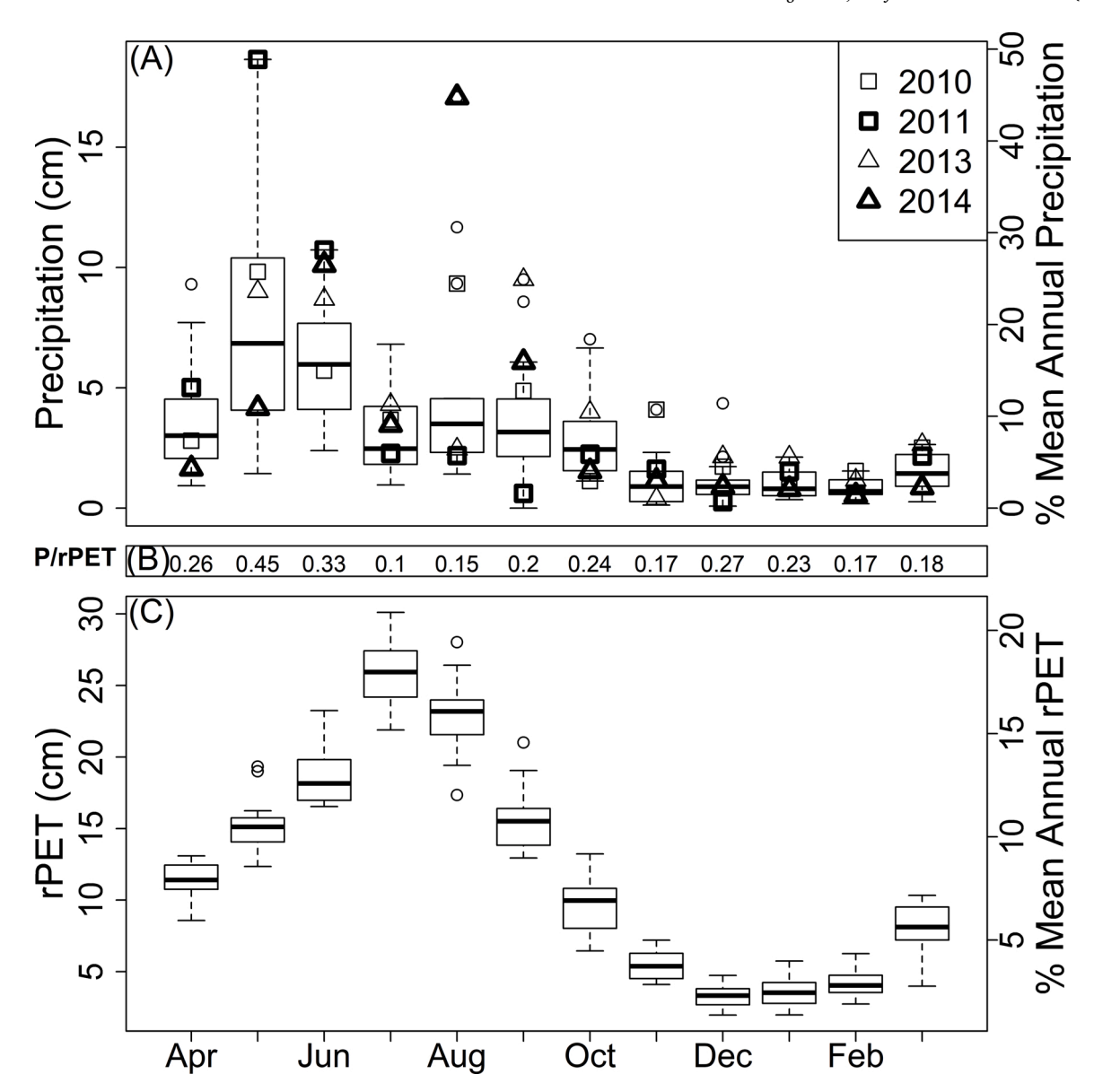


**Fig. 2.** Monthly precipitation and reference potential evapotranspiration (rPET). (A) monthly precipitation at CARC (WRCC Gage: 245761) for the modeling period (2001-10-01 to 2017-03-31). Symbols for top four precipitation years are noted in the legend. (B) Ratio of monthly median precipitation over monthly median rPET. (C) monthly rPET at CARC (Agrimet Gage: MWSM) for the modeling period. Lines within boxes are medians; boxes represent the interquartile range; whiskers extend to the value furthest from the median within one interquartile range of the box.

 $10\,$  cm square columns. Total depth of sampling was ca.  $120\,$  cm, depending on the depth to gravel. Nitrate pools in the gravel layers were much lower than in the fine textured horizons and are not presented. Soils were weighed in the field, chilled during transport to the lab, and then frozen until analyzed. Solutes were extracted from weighed subsamples with  $1\,$  M KCl and the resulting solutions were analyzed for nitrate concentration by cadmium reduction and colorimetry (Lachat, QuickChem 8500). The mass of nitrate-N per unit area (kg N ha $^{-1}$ ) and the volume of soil water per unit area (cm) were determined using wet and dry mass, measured nitrate-N concentrations, and bulk density.

Soil water sampling was conducted using tension lysimeters (PTFE/silica; Prenart Equipment; Frederiksberg, Denmark). Eighteen lysimeters were installed in Fields B and C at the bottom of the fine-textured soil (depths ranging from 40 to 120 cm), and where conditions were representative of overall field management. Lysimeters were visited one to three times per month during wetter conditions. Approximately 100 kPa of tension was applied with a hand pump to one-liter sample bottles attached to lysimeters and any water in the bottle was collected within

48 h after applying the tension. A total of 550 water samples were collected from lysimeters over a period of four years (2013–2016). Samples larger than 2 mL (319 samples) were analyzed by ion chromatography (Dionex, ICS-2100, AS18 column) and/or cadmium reduction and colorimetry (Lachat, QuickChem 8500; Seal, QuAAtro). Nitrate concentrations for each lysimeter were aggregated by monthly mean. The threshold for outlier concentrations within each 2-yr sequence was calculated as three times the interquartile range (IQR) plus the value for the 75th percentile, and outliers above this threshold were not included in the analysis. Tests for differences in lysimeter nitrate concentration among 2-yr sequences were conducted with paired Kruskal-Wallis rank sum analyses using R statistical software (kruskal-test function; R version 3.4.3; The R Foundation for Statistical Computing, Vienna, Austria).

## 2.4. Model description

Simulations of soil water movement with Hydrus-1D were used to

	Rotational	Year 3 (previous)	Year 1	Year 2	Year 3	
Rotation	Sequence	Crop (2-yr Sequence)	Crop (2-yr Sequence)	Crop (2-yr Sequence)	Crop (2-yr Sequence)	
	Fa-WW-SG	Spring Grain (Crop- <u>Crop)</u>	Fallow (Crop- <u>Fallow)</u>	Winter Wheat (Fallow- <u>Crop)</u>	Spring Grain (Crop- <u>Crop)</u>	0.5
With- Fallow	SG-Fa-WW	Winter Wheat (Fallow- <u>Crop)</u>	Spring Grain (Crop- <u>Crop)</u>	Fallow (Crop- <u>Fallow)</u>	Winter Wheat (Fallow- <u>Crop)</u>	Γ <sup>1.0</sup>
	WW-SG-Fa	Fallow (Crop- <u>Fallow)</u>	(Fallow- <u>Crop)</u>	Spring Grain (Crop- <u>Crop)</u>	Fallow (Crop- <u>Fallow)</u>	efficie
Without -Fallow	sg-ww-sg	Spring Grain (Crop- <u>Crop)</u>	Spring Grain (Crop- <u>Crop)</u>	Winter Wheat (Crop- <u>Crop)</u>	Spring Grain (Crop- <u>Crop)</u>	Crop Co.
	sg-sg-ww	Winter Wheat (Crop- <u>Crop)</u>	Spring Grain (Crop- <u>Crop)</u>	Spring Grain (Crop- <u>Crop)</u>	Winter Wheat (Crop- <u>Crop)</u>	1.0 -0.5
	ww-sg-sg	Spring Grain (Crop- <u>Crop)</u>	Winter Wheat (Crop- <u>Crop)</u>	Spring Grain (Crop- <u>Crop)</u>	Spring Grain (Crop- <u>Crop)</u>	1.0 -0.5
			AMIJJAISIOINDIJEM	AMJJASONDJEM Months	AMJJJAISIOINIDIJIFIM	Ī

Fig. 3. Crop rotations. The two crop rotations with the three associated rotational sequences of fallow (Fa), winter wheat (WW), and spring grain (SG). The first year for each phase is the year 2000 (for example, with-fallow phase Fa-WW-SG is fallow in 2000, 2003, 2006, etc.). The crop for each year is listed along with the 2-yr crop sequence in parentheses, indicating crop versus fallow for the current year (underlined) and the previous year. The gray polygons are the transpiration coefficients and the black lines are evaporation coefficients for scaling and dividing rPET into evaporation and transpiration. Coefficient values correspond to the y axes on the right side of the figure. The WW-SG-Fa rotation was fallow in 2014, which is the land use year represented in Fig. 1C where fallow fields are in black.

assess the potential response of deep percolation to crop rotation, soil architecture, and precipitation. Deep percolation is defined as water exiting the lower boundary of the model. The lower boundary of the model was simulated at a depth of 1.75 m so that it was deeper than rooting depth and was 25 cm below the deepest simulated  $z_f$  value (150 cm), to avoid possible water flux anomalies occurring near the simulated soil texture transition. Simulated deep percolation was multiplied by the median observed nitrate concentration for each 2-yr sequence to assess potential rates of nitrate leaching. Modeling included various rotational sequence and  $z_f$  values applied over the model period for which daily meteorological data were available (2001-10-01 to 2017-03-31). The first 17 months of simulation were used as a spin-up period to establish appropriate initial conditions specific to each rotational sequence before the start of the 14-yr model reporting period (2003-04-01 to 2017-03-31). We report the mean annual results aggregated over the model reporting period. For all simulations, the model was driven by precipitation data from the WRCC weather station and rPET data from the Agrimet station. Agrimet rPET values were calculated with the Kimberly-Monteith method, which uses an established perennial grass without water limitation as the reference crop (Dockter and Palmer, 2008). Potential evapotranspiration was allocated completely to potential transpiration when a crop was present and completely to potential evaporation when a crop was absent. Potential transpiration rates for winter wheat and spring grain were calculated by scaling rPET with crop coefficients. Crop coefficients were calculated based on crop growth stage estimated from growing degree day C and the ratio of actual ET (measured by eddy covariance) to rPET when crops were growing (Sup Table 2.4b; Sup Section 2.4; Sup Figs. 2.4d and 2.4e; Vick et al., 2016). Potential evaporation rates were calculated by scaling rPET with a fallow coefficient, which was estimated as the ratio of actual ET (measured by eddy covariance) to rPET during fallow periods (Sup Fig. 2.4f). Maximum rooting depth was informed by soil pit observations and root growth rates were estimated as a function of cumulative growing degree days after seeding. The root growth rate function

followed the approach of Thorup-Kristensen et al. (2009) with rate adjusted based on preliminary simulation results (Sup Table 2.4b; Sup Section 2.4).

The Hydrus model was configured with two materials to simulate soils commonly observed in the study area: a shallow fine-textured horizon overlying a deeper coarse-textured horizon. The van Genuchten soil hydrology parameters used for the lower horizon were the default values for sand from Rosetta Lite v. 1.1 embedded in Hydrus (parameters listed and defined in Sup Table 2.4a). For the upper fine-textured horizon, the residual water content value ( $\theta_R$ , 0.12) was based on volumetric water content (VWC) measured in soils near wilting point and the saturated water content value ( $\theta_s$ , 0.5) was based on porosity calculated from bulk density measurements (Sup Table 2.4a). A value of 0.5 was used for the pore connectivity parameter l (Mualem, 1976). Remaining van Genuchten parameters for the fine-textured horizon were set to default values for clay loam from Rosetta Lite v. 1.1. Volumetric water content at field capacity for the fine-textured soil horizon was calculated to be 0.33 within Hydrus according to Twarakavi et al. (2009). Deep percolation can occur at VWC below field capacity (Twarakavi et al., 2009; Flury et al., 1994), but we apply a simplification and define soils as primed for deep percolation when simulated daily VWC (at a depth 2 cm shallower than the  $z_f$  depth) was greater than field capacity. Maximum soil water storage potential was estimated as the difference between field capacity and wilting point for the fine-textured horizon multiplied by  $z_f$ . Precipitation storage efficiency was calculated as the fraction of measured annual precipitation that was not lost to modeled deep percolation, evaporation, or runoff in fallow years.

The influence of fine-textured soil horizon thickness on soil water storage capacity and deep percolation was assessed by varying  $z_f$  from 5 to 150 cm (encompassing values observed in all but one soil pit) in increments of 5 cm (30  $z_f$  values). The hydrologic effect of fallow on deep percolation was assessed using model scenarios simulating the six rotational sequences depicted in Fig. 3, such that all combinations of rotational sequence and annual weather were represented. Thirty  $z_f$ 

values for each of six rotational sequences produced a total of 180 model simulations.

To assess whether the model produced reasonable predictions of soil water content dynamics, additional simulations were configured for comparison to field observations and coefficients of determination ( $R^2$ ) were calculated for simulated versus observed values (Sup Section 2.4). The sensitivity of model results was manually assessed for different values of: scaling of mean annual precipitation, maximum root depth, root growth rate, fallow crop coefficient, spring grain seeding date, crop development rates, and van Genuchten parameters for the fine-textured horizon (10 texture scenarios assessed; Sup Table 2.4e).

#### 3. Results

#### 3.1. Soil water content and soil nitrate

Soil water contents observed during August and September of fallow years were consistently higher than those observed following harvest (Fig. 4A). Volumetric water content in fallow soils was up to 0.18 higher than post-harvest across 15-cm depth increments. The total water stored in soil to a depth of 105 cm was 10.1 cm post-harvest and 23.3 cm in fallow (Fig. 4A). Total nitrate-N pools (kg N ha $^{-1}$ ) in the top 15 cm of soil were seven times higher in fallow than post-harvest and total nitrate-N pools in deeper soils were at least three times greater in fallow than post-harvest for all but the deepest 15-cm increment. The total mass of soil nitrate-N to a depth of 105 cm was 12 kg ha $^{-1}$  after harvest and 46 kg ha $^{-1}$  during fallow (Fig. 4B). Apparent dissolved nitrate-N concentrations (mg L $^{-1}$ ; calculated as nitrate-N pool from soil extractions / water

pool) were 1.3–2 times higher in fallow than post-harvest for all but the deepest profile increment (Fig. 4C). The depth-weighted mean nitrate-N concentrations over the profile were 12 mg  $\rm L^{-1}$  for post-harvest and 19 mg  $\rm L^{-1}$  for fallow.

Nitrate-N concentration values observed in lysimeter samples over the 2013–2016 period ranged from 0.03–347 mg N L $^{-1}$ . Six values from one field in the Crop-Fallow sequence were removed as extreme outliers reducing the maximum value to 45.5 mg N L $^{-1}$ , with a median of 12.0 mg N L $^{-1}$  (IQR 8.1–20.2 mg N L $^{-1}$ ). Median concentrations were significantly higher for Fallow-Crop years (19.4; IQR 9.9–28.0 mg L $^{-1}$ ) than for Crop-Fallow years (9.8; IQR 6.1–15.7 mg L $^{-1}$ ; p < 0.05) and Crop-Crop years (11.1; IQR 7.6–17.5 mg L $^{-1}$ ; p = 0.06; Table 1). Lysimeter nitrate concentrations did not vary with  $z_f$  (R $^2$  = 0.01, p = 0.33; Sup Fig. 3.1a).

#### 3.2. Spatial distribution of soil thickness $(z_f)$

Soil pits in Field B (n = 18) had  $z_f$  values ranging from 26 to greater

**Table 1** Lysimeter nitrate concentrations. Summary statistics for lysimeter nitrate-N concentrations (mg  $L^{-1}$ ) with extreme outliers removed.

2-yr Sequence	Mean	StDev	Median	0.25 and 0.75 Quartiles	Sample Size
Crop-Crop	14.0	9.3	11.1	7.6, 17.5	34
Crop-Fallow	11.2	6.4	9.8	6.1, 15.7	23
Fallow-Crop	19.9	13.0	19.4	9.9, 28.0	36

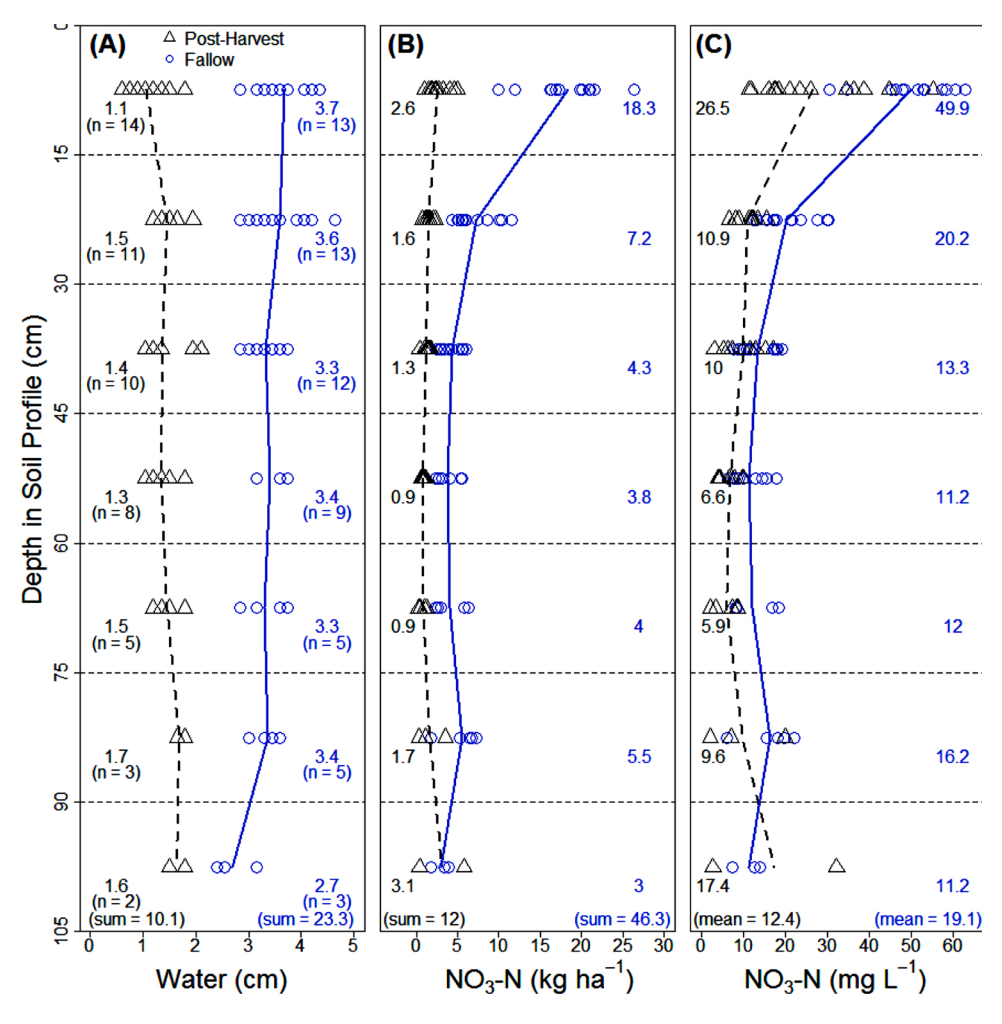


Fig. 4. Soil water and nitrate profiles by crop sequence. (A) Water pools for soil profile samples collected at 15 cm increments in August and September 2012 in fields fallow for a year (blue) and fields immediately post-harvest (black). Values on left side of the plot for each depth increment are mean water pools for samples post-harvest and values in parentheses are sample sizes. Values on the right are parallel for fallow field samples. Black dashed line is mean values for post-harvest and blue line is mean values for fallow. (B) Nitrate pools for the same samples in panel A with parallel symbology and mean values by depth increment. Sum of profile means are at the bottom. (C) Apparent nitrate concentrations calculated with nitrate and water pools from panels A and B with symbology and mean values parallel to panel A. Mean of profile means are at the bottom. (For interpretation of the references to colour in this figure legend, the reader is referred to the web version of this article).

than 142 cm ( $z_f$  transition not observed in one pit, 142 cm deep; Sup Table 3.2a), with a median value of 48 cm. This field is primarily mapped as Danvers-Judith complex, with series descriptions suggesting a  $z_f$  range from 58–150 cm with mean  $z_f$  values for the two series of 61 and 131 cm (Sup Table 2.2a). Additionally, a portion of Field B includes Tamaneen series, which is described as having a minimum  $z_f$  of 43 cm.

The  $z_f$  measured in soil pits from Field C (n = 26) ranged from 16 to 125 cm with a median value of 86 cm. In this field, values of  $z_f$  up to 55 cm (n = 9 soil pits) showed a positive relationship with NDVI from the 2011 NAIP image ( $R^2 = 0.46$ ; Fig. 5B). Soil pits with  $z_f$  values greater than 55 cm all had NDVI values near 0.15, so extrapolation of the z<sub>f</sub>. NDVI relationship was inappropriate for deeper soils. A subsequent soil core sampling campaign targeting validation of this relationship found 68 of 72 core locations falling within the NDVI-predicted  $z_f$  value category (Sup Section 3.2). This field is mapped as a Doughty-Sipple-Judith complex. The Doughty, Sipple, and Judith series have mean  $z_f$  values of 81, 132, and 61 cm respectively, with a range of 51-152 cm across the three series (Sup Table 2.2a). Lower values for  $z_f$  observed in pits (on both Fields B and C) and across Field C based on the  $z_f$  relationship to NDVI suggest that soil mapping for the fields do not capture the thinnest fine-textured soils, nor do they characterize the distribution of  $z_f$ necessary for mechanistic hydrologic modeling. We adopted an example  $z_f$  distribution ("standard- $z_f$ ") with mean  $z_f$  of 50 cm based on NDVI for Field C and soil pits on Field B, and standard deviation of 30 cm based on soil pits in both fields.

#### 3.3. Model results versus observations and sensitivity

The model explained 72 % (i.e.  $R^2=0.72$ ) of the variation in observed VWC during winter wheat and spring grain years, 53 % of variation in observed ET during the winter wheat year, 19 % of variation in observed ET during the spring grain year, and exhibited a negative coefficient of determination ( $R^2$ ) with observed ET during the fallow

year (i.e., the chosen parameterization did not allow the mechanistic model to outperform the statistical mean during fallow,  $R^2 = -0.28$ ; Sup Fig. 3.3a). Fallow year ET was calculated by scaling rPET with a coefficient (i.e. the fallow coefficient) that was empirically derived from the median ratio of measured ET to rPET (0.22). While simulations with a fallow coefficient value of 0.22 reproduce the variation in moderate ET rates reasonably well, the highest ET rates could not be reproduced by simulations constrained by that value, resulting in a negative R<sup>2</sup> value. The implications of these episodically higher evaporation rates measured during fallow (Sup Fig. 2.4f) were evaluated with sensitivity analysis scenarios where the fallow coefficient was set to 0.5 (scenario 24; Sup Table 3.3a). Simulation results with the higher fallow coefficient produced patterns similar to the primary simulation, but with decreased PSE, time above field capacity, overall deep percolation, and difference in deep percolation between crop and fallow years; the higher fallow coefficient increased the fraction of deep percolation occurring on thinner soils. More broadly, the sensitivity analysis identified the rescaling factor for precipitation and the fallow coefficient as the parameters with the most influence on simulated water movement and that general patterns in model results were robust across likely parameterization scenarios.

#### 3.4. Simulated precipitation partitioning

Model results suggest that shallower fine-textured soil horizons spend a larger fraction of time with VWC above field capacity, representing soils that are more regularly "primed" for deep percolation ( $z_f$  of 25 cm = 39 % of time primed,  $z_f$  of 50 = 33 %, and  $z_f$  of 100 = 24 %; Sup Figs. 3.4b-d). Thinner soils spending more time primed for water loss resulted in higher rates of deep percolation for thinner  $z_f$  soils (Figs. 6 and 7). Simulated mean annual deep percolation rates varied more across  $z_f$  values (within a 2-yr sequence) than among 2-yr sequences for any given  $z_f$  value. The range of simulated deep percolation rates across

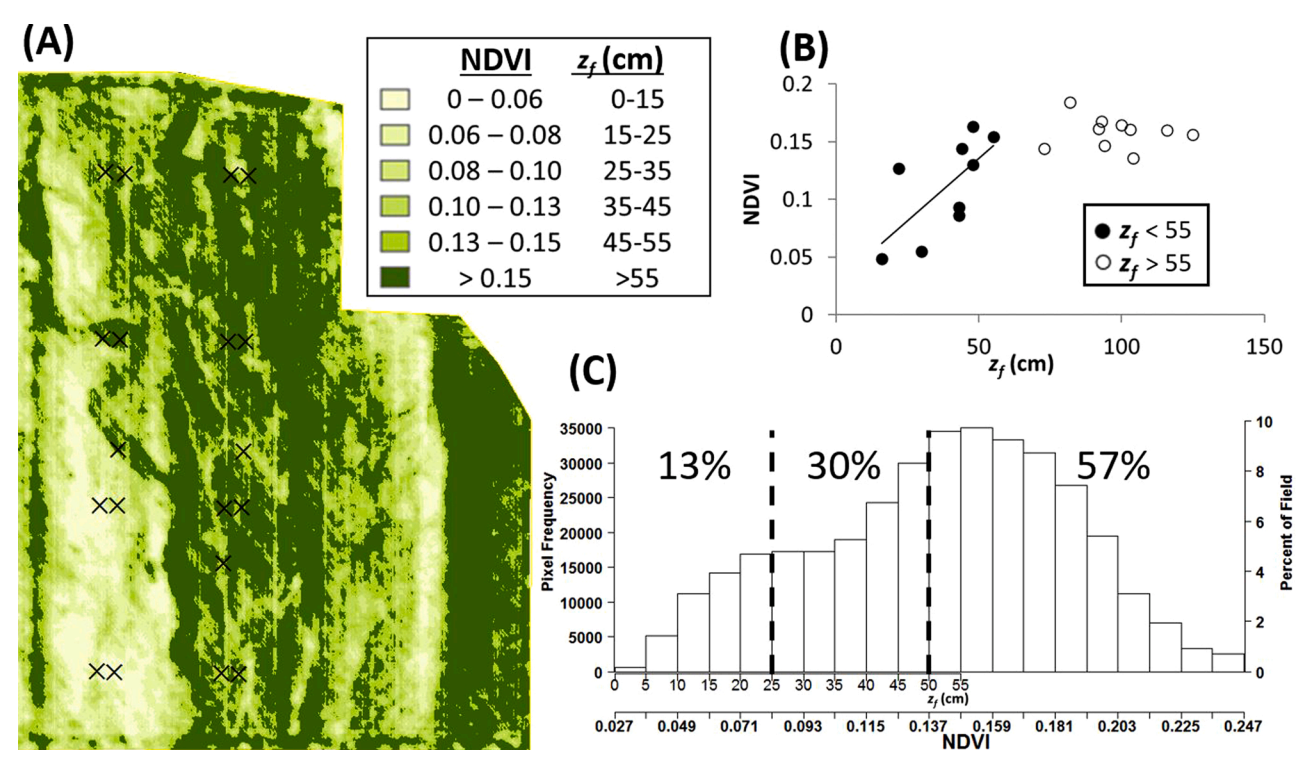


**Fig. 5.** Normalized Difference Vegetation Index (NDVI) and thickness of fines ( $z_f$ ). (A) NDVI values calculated for Field C using a one-meter resolution National Agricultural Imagery Program (NAIP) image captured on July 24, 2011. Cross symbols are locations of soil pits excavated in 2012. (B) Relationship between mean NDVI for pixels touching a two-meter radius around soil pits and  $z_f$  observed in the pit. Black line represents linear regression line, described in detail in Sup Section 3.2. (C) Pixel frequency histogram for NDVI values and corresponding  $z_f$ . Values near top of the plot are the percent of the field in depth categories separated by dashed lines (0-25, 25-50, >50 cm).

 $z_f$  values was largest for the Crop-Fallow sequence with a spread of 13.6 cm yr $^{-1}$  (2.8–16.4 cm yr $^{-1}$ ; Fig. 7A; Table 2). The range in deep percolation rates across  $z_f$  values was 7.9 cm yr $^{-1}$  for Fallow-Crop (1.9–9.7 cm yr $^{-1}$ ) and 10.9 cm yr $^{-1}$  for Crop-Crop (0.6–11.6 cm yr $^{-1}$ ). The difference in deep percolation rates among 2-yr sequences was largest (6.9 cm yr $^{-1}$ ) between Crop-Fallow and Fallow-Crop for  $z_f = 30$  cm and the range across 2-yr sequences was smallest (2.2 cm yr $^{-1}$ ) at the largest  $z_f$  values. The dependence of deep percolation on  $z_f$  was strongest at lower  $z_f$  values (< 100 cm), while deep percolation was relatively insensitive to  $z_f$  at higher values (> 100 cm).

Across 2-yr sequences, the thinnest soils ( $z_f$  < 25 cm, Fig. 6) had 14-yr mean simulated water loss rates approximately equal to mean annual precipitation (38 cm yr $^{-1}$ ) indicating that on average, no net precipitation storage occurred regardless of crop presence/absence. Mean PSE during Crop-<u>Fallow</u> years (white space below 38 cm line in Fig. 6B) for the model reporting period plateaued at a maximum value of 9.1 cm, or 23 % of mean annual precipitation (Sup Table 3.4a). The mean PSE for Crop-<u>Fallow</u> given the standard- $z_f$  distribution was 8%. The maximum annual PSE during our modeling period was 46 % for the thickest soils ( $z_f$  = 150) in 2013 when 22.3 of the 48 cm of annual precipitation was stored, a value 71 % of theoretical maximum of 31.5 cm (0.21 VWC times 150 cm; Sup Fig. 3.4e).

Simulated transpiration rates during Fallow-Crop years were higher with deeper  $z_f$ , resulting in mean annual combined losses exceeding mean annual precipitation by up to 9.5 cm yr $^{-1}$  for the thickest soils (Fig. 6C; Table 2). This increased loss of stored water with increasing  $z_f$  in Fallow-Crop years mirrors the increase in water storage (PSE in Fig. 6B) with increasing  $z_f$  in Crop-Fallow years. The simulated mean annual transpiration rates for thickest soils ( $z_f = 150$  cm) in Fallow-Crop years (34.6 cm yr $^{-1}$ ) were approximately 10 cm higher than rates in Crop-Crop years (24.5 cm yr $^{-1}$ ), due to the water stored during fallow years. The transpiration rate difference between cropped years was less pronounced for thin soils ( $z_f \le 25$  cm), where mean annual simulated transpiration was 16.5 cm yr $^{-1}$  in Fallow-Crop years and 13.0 cm yr $^{-1}$  in Crop-Crop years.

While annual deep percolation was strongly correlated with annual precipitation for the thinnest soils ( $z_f = 10 \text{ cm}$ ;  $R^2 = 0.77$ , p < 0.005), this relationship breaks down with increasing  $z_f$ . For soils with  $z_f > 40 \text{ cm}$ , less than 33 % of annual deep percolation was independently explained by annual precipitation (Sup Fig. 3.4a); the rate and timing of precipitation in the current and previous year were also important

explanatory variables for precipitation partitioning. For example, 2010 and 2011 had virtually identical annual precipitation (47.8 and 47.6 cm respectively), but 2010 had only 4.6 cm of deep percolation ( $z_f = 50$ ) in contrast to 24.4 cm in 2011. Higher deep percolation in 2011 occurred due to above normal precipitation occurring prior to peak rPET, on soils with high antecedent VWC from above average precipitation the preceding fall (Figs. 2 and 8; Sup Section 3.4).

#### 3.5. Nitrate leaching

As a result of the modeling approach, the shape of the relationship between simulated nitrate leaching and  $z_f$  (Fig. 7C) was identical to that for deep percolation (Fig. 7A) for each 2-yr sequence, but nitrate leaching rates were shifted relative to deep percolation due to different nitrate concentrations observed for each 2-yr sequence (Table 1). Modeled nitrate leaching rates were lowest in the Crop-Crop sequence, which has the lowest deep percolation rates and intermediate nitrate concentrations. The Crop-Fallow sequence had the highest modeled nitrate leaching rates for mid-range  $z_f$  values, but at low and high  $z_f$  values the Fallow-Crop sequence had the highest leaching rates.

Simulated deep percolation and nitrate leaching rates for all three rotational sequences with fallow were higher than rates for all three rotational sequences without fallow (Fig. 7B and D). While all rotational sequences without fallow group tightly across  $z_f$  values for deep percolation and nitrate leaching, the three rotational sequences with fallow have variable deep percolation and nitrate leaching rates for the same  $z_f$  value. Mean nitrate leaching rates for the two rotations differ by 3.8 kg ha<sup>-1</sup> yr<sup>-1</sup> at low  $z_f$  values, but the difference decreases to 2.0 kg ha<sup>-1</sup> yr<sup>-1</sup> at  $z_f$  values greater than 100 cm (Fig. 7D). The  $z_f$  weighted difference between the rotations (assuming standard- $z_f$ ) was 2.8 kg N ha<sup>-1</sup> yr<sup>-1</sup> (without-fallow = 4.2; with-fallow = 7.0 kg N ha<sup>-1</sup> yr<sup>-1</sup>). Overall nitrate leaching rates for the rotational sequences range from 0.2 kg N ha<sup>-1</sup> yr<sup>-1</sup> for thick  $z_f$  soils in without-fallow rotational sequences to 16.9 kg N ha<sup>-1</sup> yr<sup>-1</sup> for thin  $z_f$  soils in with-fallow rotational sequences.

#### 3.6. Scaling simulation results to fields and landforms

While only 43 % of Field C has  $z_f < 50$  cm (Fig. 5C), model results indicate 61 % of deep percolation and 59 % of nitrate leaching occurs through those thinner soils (Table 3; Sup Fig. 3.6a). The fraction of the field with  $z_f < 25$  cm (13 %) accounts for 25 % of the mean annual deep

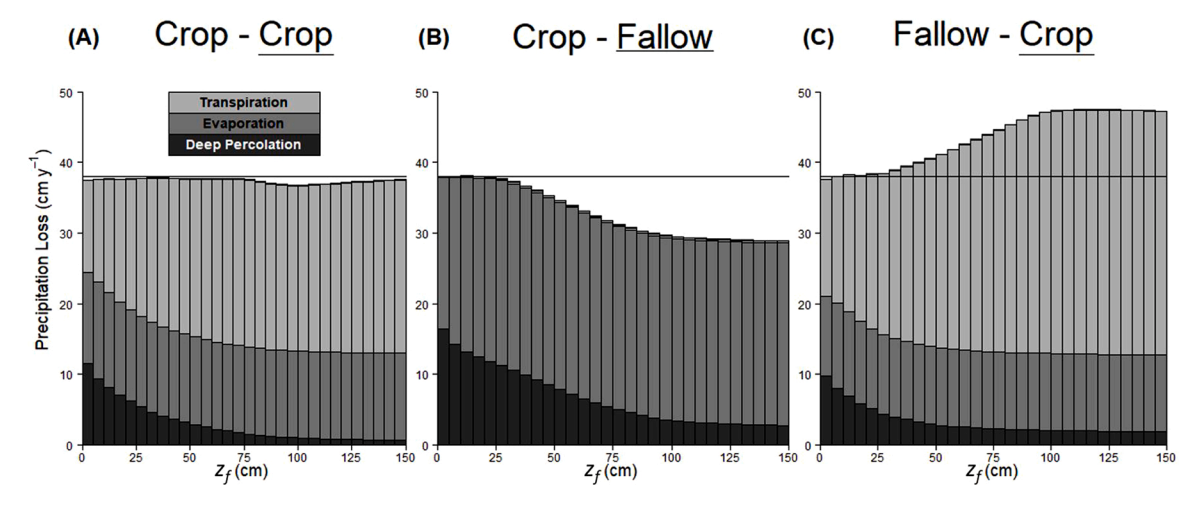


Fig. 6. Simulated precipitation partitioning by 2-yr crop sequence. Mean annual precipitation partitioning results for 14-y model reporting period for the three withfallow rotations. Each bar represents mean 14-y water loss to transpiration, evaporation, and deep percolation, with total bar height representing total losses (cm). Bar heights greater than 38 cm indicate mean annual losses exceeding 14-y mean annual precipitation and include losses of water stored from the previous year. (A) is data from model years from the Crop-Crop sequence (field is in crop and was crop last year). (B) is data from fallow years (Crop-Fallow). Total values less than 38 cm (white area below line) indicate annual precipitation exceeding losses, and thus precipitation is stored for the following year. (C) is data from the Fallow-Crop sequence.

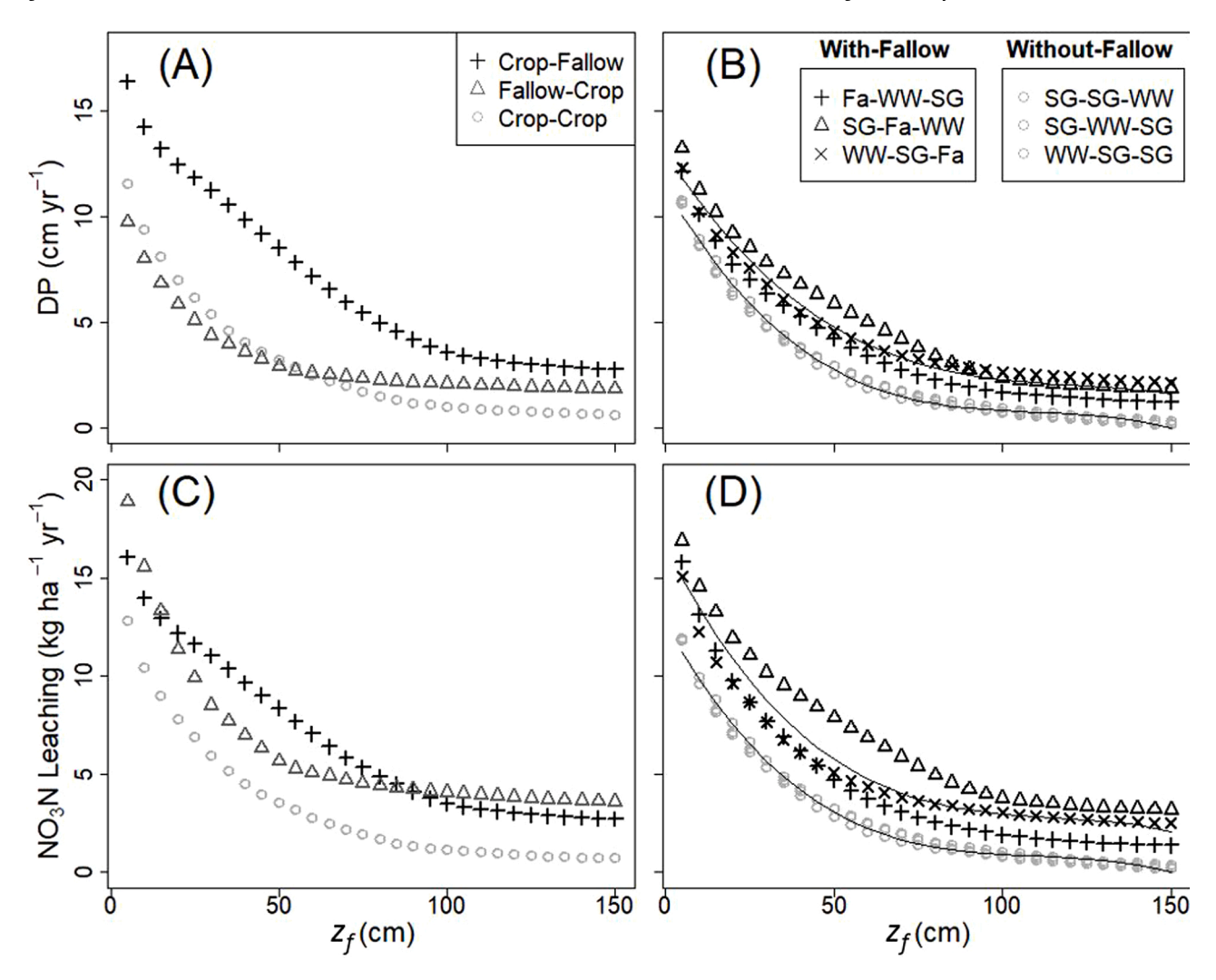


Fig. 7. Deep percolation (DP) and nitrate leaching versus thickness of fines( $z_f$ ). (A) 14-yr mean DP versus  $z_f$  aggregated by crop sequence. This is the same DP data in Fig. 6. (B) 14-yr mean DP versus  $z_f$  aggregated by crop rotation. Lines are third degree polynomial relationships for mean DP aggregated by rotation type (with-fallow and without-fallow; Sup Table 3.4b). (C) 14-yr mean nitrate leaching versus  $z_f$  aggregated by crop sequence. (D) 14-yr mean nitrate leaching versus  $z_f$  aggregated by rotation. Lines are third degree polynomial relationships parallel to panel B.

**Table 2** Summary of precipitation partitioning by sequence. Maximum, minimum, and range of mean annual partitioning losses (cm yr $^{-1}$ ) across  $z_f$  values, presented as bar heights in Fig. 6. Runoff values were all <=0.1 and are not shown. Small values for transpiration in the Crop-Fallow sequence are due to modest early season growth of winter wheat prior to 1 April, which is aggregated within the Crop-Fallow sequence.

Sequence	Evaporation			Transpira	Transpiration			Deep Percolation			Total Losses		
	Min	Max	Range	Min	Max	Range	Min	Max	Range	Min	Max	Range	
Crop-Crop	12.3	13.6	1.3	13.0	24.5	11.6	0.6	11.6	10.9	36.8	37.8	1.0	
Crop-Fallow	21.5	26.6	5.1	0.1	0.2	0.1	2.8	16.4	13.6	29.0	38.1	9.2	
Fallow-Crop	10.9	12.1	1.2	16.5	34.6	18.1	1.9	9.7	7.9	37.6	47.5	9.9	

percolation, while field areas with  $z_f$  of 25–50 cm and > 50 cm account for 36 % and 41 % of deep percolation, respectively. The Crop-Fallow sequence represents one-third of the time in the 3-yr rotation but produces 55 % of the deep percolation and 43 % of nitrate leaching (Table 3). The model approach produces similar distributions of deep percolation and nitrate leaching across the field, the largest difference being the larger fraction of nitrate leaching occurring in Fallow-Crop years (35 %) relative to deep percolation (23 %) occurring in those years (Table 3, Fig. 9, Sup Fig. 3.6a). This difference in nitrate leaching is due to the higher nitrate concentration accumulated from mineralization during fallow years and resulting from fertilizer application during crop years (Table 1).

Application of the deep percolation and nitrate leaching rate relationships to  $z_f$  for the with-fallow rotation (upper polynomial line in Fig. 7B and D) to various observed  $z_f$  distributions produced a range of estimates presented in Table 4. The combinations of  $z_f$  distributions and model time periods produce deep percolation rates ranging from  $2.0-10.8~{\rm cm~yr}^{-1}$  and nitrate leaching rates ranging from  $2.2-13.8~{\rm kg~N}$  ha<sup>-1</sup> yr<sup>-1</sup>.

#### 4. Discussion

Periods of fallow in a dryland crop rotation interacted with both rainfall and variation in soil water storage capacity to exert a strong

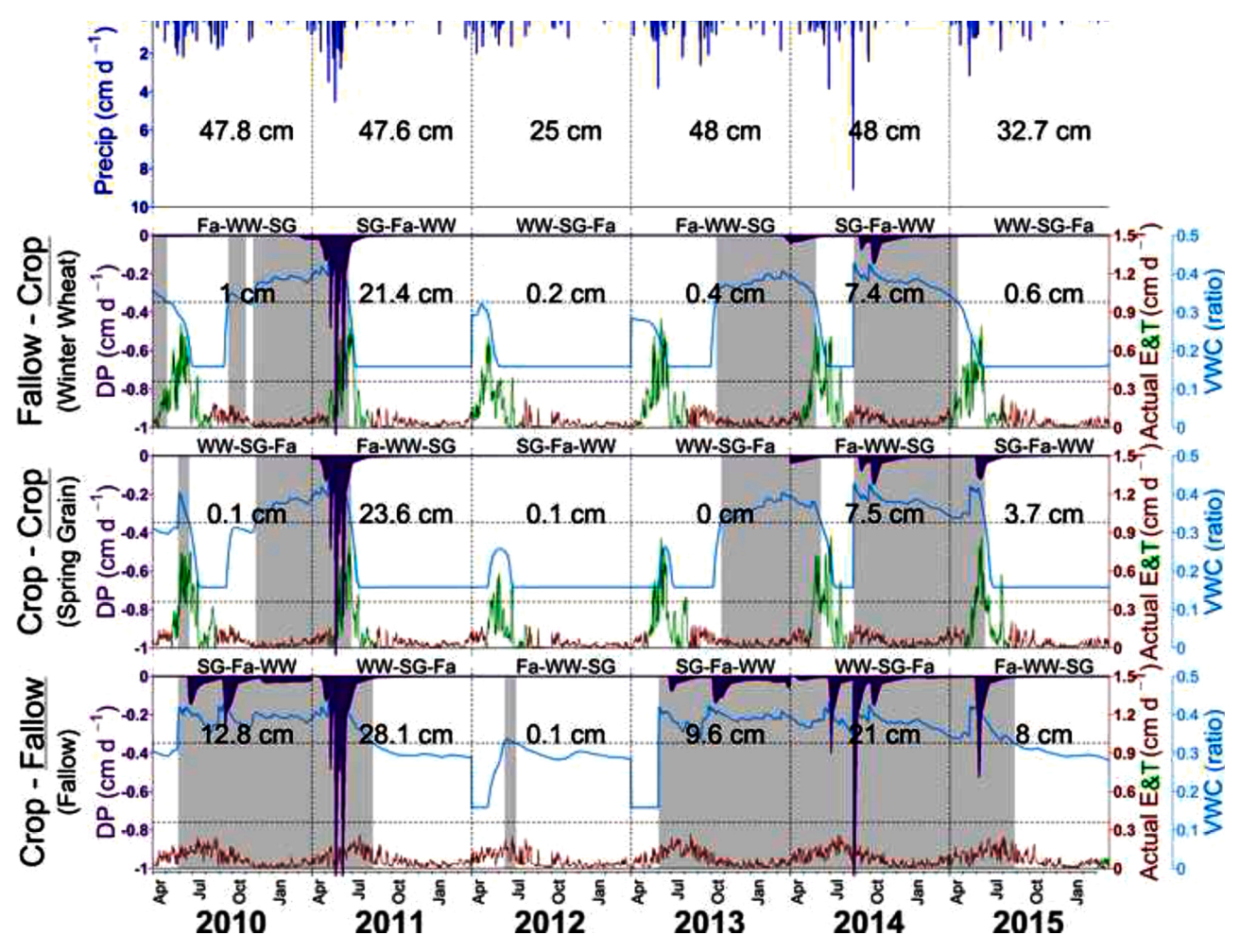


**Fig. 8.** Modeled daily deep percolation (DP), transpiration (T) and evaporation (E). The top panel is daily precipitation from CARC (WRCC Gage: 245761); the value for each year is the annual precipitation total. The bottom three panels are model results for  $z_f$  of 50 cm, organized by crop sequence year with rotations printed above for each year. Values printed in the panels are the annual DP (cm yr<sup>-1</sup>). Purple polygons represent DP and correspond to the left axis. Blue lines represent soil volumetric water content (VWC) and correspond to the second right axis. Shaded areas represent VWC greater than field capacity (hydrologically primed for deep percolation). Green lines represent T and correspond to the right axis. Black lines represent E and correspond to the right axis. Extended versions of this plot with all model years for different  $z_f$  values are included in the supplemental materials. (For interpretation of the references to colour in this figure legend, the reader is referred to the web version of this article).

influence on patterns of simulated episodic nitrate leaching. We suggest that the first step in predicting leaching is to understand the controls on partitioning of precipitation to soil storage, evapotranspiration, and deep percolation. Subsequently, we develop the concept that more intense precipitation on wetter soils defines hydrologic hot moments of deep percolation. Wet soil conditions promote accumulation of nitrate mineralized from soil organic matter, contributing to biogeochemical hot moments of potential leaching. Areas with thinner soils exceed field capacity more frequently, hence defining hot spots for deep percolation. Hot moments of meteorological phenomena interact with hot spots of low soil water storage capacity to define ecological control points that can be used to predict the episodic nature of deep percolation and nitrate leaching across the system. The ability to predict nitrate leaching control points suggests management practices that may help to increase N use efficiency, and points to future research that may further inform sustainable farming practices.

# 4.1. Controls on precipitation partitioning

Our simulation results for a dryland system demonstrate the interactions of weather, crop rotation, and thickness of fine-textured soil horizons  $(z_f)$  as primary controls on the partitioning of precipitation in

soils. Weather and land use exert control on partitioning by altering the timing of supply and demand for meteoric water, while  $z_f$  determines the size of the storage buffer that can retain soil water against gravity, allowing for subsequent use by plants or loss via evaporation.

A motivation for the practice of fallow is to store water for the subsequent crop, an outcome that our model results suggest is controlled primarily by spatial variation in the thickness of fine-textured surface soil, a proxy for water storage potential ( $z_f$ , Figs. 6 and 7). Our 14-yr mean modeled PSE values (range: 0–23%;  $z_f$  weighted mean: 8%) were low relative to values of 15–45 % compiled by Nielsen et al. (2005), a result consistent with the relatively low water holding capacity of study area soils. We found that the highest deep percolation rates tend to be associated with thinner  $z_f$  (Fig. 7), which is parallel to Wang et al. (2009) who found that deep percolation was negatively correlated with soil water storage potential related to variation in soil texture.

Within limits dictated by soil water storage potential, factors affecting gains and losses of water exert important controls on PSE and may include tillage/stubble management, crop type, fallow duration (Nielsen et al., 2005), and timing of precipitation. The maximum PSE observed during our modeling period (46 %) occurred in 2013, when unusually high precipitation rates occurred in the months after peak rPET (Fig. 2). Under more typical conditions when the highest

Table 3

Field scale deep percolation (DP) and leaching. Percentage of DP and leaching for the mean 3-yr with-fallow rotation attributed to each 2-yr sequence for thin (0-25 cm), intermediate (26-50 cm) and thick (> 50 cm) thickness of fines ( $z_f$ ) soils on Field C. The bottom row is the percentage of 3-yr DP and leaching attributed to each  $z_f$  category. Percentages in parentheses are the portion of the field area in that depth range. Subtle deviations from 100 % in sum of bottom row values and sum of right column values within DP and leaching are due to rounding.

	Deep Percolat	ion			Leaching				
Period within Rotation	0-25 cm (13 %)	26-50 cm (30 %)	> 50 cm (57 %)	All depths	0-25 cm (13 %)	26-50 cm (30 %)	> 50 cm (57 %)	All depths	
Crop-Crop	7%	9%	8%	24 %	6%	8%	7%	21 %	
Crop-Fallow	12 %	19 %	24 %	55 %	9%	15 %	19 %	43 %	
Fallow-Crop	6%	8%	9%	23 %	9%	12 %	14 %	35 %	
Full Rotation	25 %	36 %	41 %		24 %	35 %	40 %		

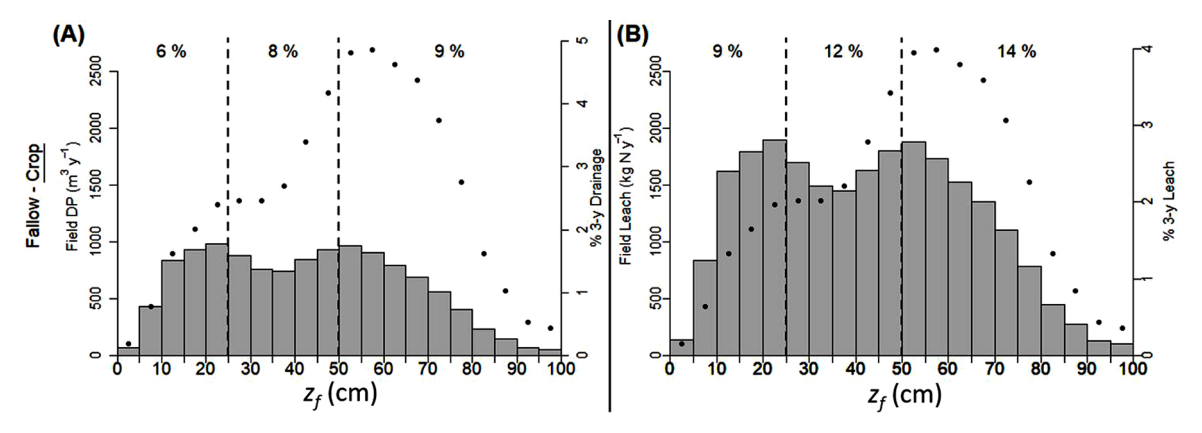


**Fig. 9.** Field scale simulated deep percolation (DP) and leaching for Field C. (A) Mean DP volume for the full field area by thickness of fines  $(z_f)$  for the Fallow-Crop sequence. Each bar is the mean annual DP of three with-fallow rotations, for the 14-y model reporting period. Values near the top of the plots are the percent of the total DP volume summed over the three crop sequence years for the 0-25, 25-50, and 50-100 cm  $z_f$  ranges. (B) Mean nitrate leaching mass for the for the full field area, configured parallel to DP in panel (A). Black dots show the relative distribution of  $z_f$  of Field C (bar heights in Fig. 5C). See supplemental materials for parallel plots for all 2-yr crop sequences.

Table 4
Deep percolation (DP) and leaching by thickness of fines  $(z_f)$  distribution and time period. DP and leaching rates based on  $z_f$  distributions characterizing Field B, Field C, the Judith, and Danvers soil series for different time periods.  $z_f$  distributions are normal with the centers and standard deviations specified. DP and leaching rates for 14-yr estimates are based on relationships depicted in Fig. 7B and D for the with-fallow rotation. Rates are also provided for the abnormally wet 2011-14 period and the more average 2012-2014 period. Standard deviations for soil series were not available and are set equal to that for Field B pits.

	$z_f$ Distribution (cm)		Deep Perco	olation (cm yr <sup>-1</sup> )		Leaching (kg N ha <sup>-1</sup> yr <sup>-1</sup> )		
$z_f$ Scenario	$z_f$ center	$z_f  \mathrm{SD}$	14-yr	2011-14	2012-14	14-yr	2011-14	2012-14
Field B Pit Median	48	30	6.2	10.8	6.7	7.7	13.8	8.3
Field B Pit Mean	63	30	4.8	9.2	5.0	5.9	11.7	6.0
Field C Pit Median	86	31	3.2	7.1	3.0	3.9	9.1	3.4
Field C Pit Mean	76	31	3.8	8.0	3.8	4.8	10.2	4.5
Judith Series	61	30	4.8	9.2	5.0	5.9	11.8	6.0
Danvers Series	112	30	2.3	5.7	2.0	2.9	7.5	2.2

precipitation rates occurred in May and June, large fractions of annual precipitation were subject to high evaporative losses from fallow fields during summer months (> 0.1 cm d<sup>-1</sup>; Sup Figs. 3.4b-d). In cases of fallow during drier years (2004 and 2012) or in years preceded by above-normal fall precipitation (2011 and 2015), evaporation and/or deep percolation far exceed storage, even for soil with the thickest  $z_f$ , resulting in little to no net change in water storage over the year. Simulated evaporation during fallow years is approximately twice that of cropped years (Fig. 6; Table 2) and was influenced by the capacity of soils to transport water upward to the surface in our simulations. The simulation of upward water transport is heavily influenced by the van Genuchten pore size distribution parameter n, where the maximum upward flux potential occurs in soils with n values around 1.5 (Or et al., 2013). Values of n for clay loam soil textures (ca. 1.4) fall near the 1.5 value for maximum upward water transport potential. This suggests that clay loam soils such as those in our study area may be highly prone to evaporative losses, which can extract water efficiently to a depth of approximately 50 cm (Or et al., 2013). Our finding that water losses during fallow exceed storage agrees with previous work in the Great Plains (Peterson et al., 1996) and prompts questions about sustainability of the practice in the context of pressure to increase "crop per drop" (Rockstrom, 2003).

# 4.2. Weather & soils as controls on deep percolation and leaching

The relatively large amounts of deep percolation simulated during spring storms on wet soils (2011 versus 2010; Fig. 8) underscore the potential for relatively short periods of time to have a disproportionate effect on whole-system behavior (i.e. "hot moments" in time; McClain et al., 2003). In semi-arid climates such as our study area, where rPET exceeds precipitation on both a mean annual (148 versus 38 cm) and a mean monthly (Fig. 2) basis, soils are typically below field capacity and poised to store precipitation. Periods of relatively high intensity precipitation are necessary for soil water to exceed storage potential and

simulation results indicate that the majority of deep percolation occurs when VWC is above field capacity. These periods when VWC is above field capacity hence represent hot moments of disproportionate importance for controlling cumulative long-term groundwater recharge rates. With lysimeter nitrate-N concentrations ranging up to 45 mg  $L^{-1}$ , hot moments for deep percolation represent the temporal control points for nitrate leaching that must be quantified to understand aggregate ecosystem behavior (McClain et al., 2003; Bernhardt et al., 2017). The propensity for intense precipitation to drive export of water and solutes from soils was demonstrated by 54 % of deep percolation and 56 % of leaching over the 14-yr period occurring in just the two years associated with the largest monthly precipitations in May 2011 and August 2014 (Figs. 2, 8 and Sup Figs. 3.4b-d). As a result, a two or three year study (e. g. 2012-2014; John et al., 2017) may capture highly variable rates of deep percolation, leaching, and economic outcomes that are distinct from approaches that aggregate longer term responses (Sigler et al.,

The influence of thin fine-textured soil horizons on deep percolation suggests that even if thin soils are limited in spatial extent, they may be disproportionately important to whole-system leaching behavior (i.e. a "hot spot" in the landscape; McClain et al., 2003). Thinner  $z_f$  soils have less water holding capacity and reach field capacity more readily, hence thinner soils are primed for water loss after smaller precipitation events and may be defined as hot spots, with a propensity to exaggerate the influence of deep percolation hot moments. In fact, simulation results indicate that thinner soils spend more time primed compared to thicker soils ( $z_f$  of 25 = 38.5 %;  $z_f$  of 100 = 23.6 % time; Sup Figs. 3.4b and 3.4d). This pattern was reflected in deep percolation and nitrate leaching rates that were five times higher for  $z_f$  from 0-25 cm compared to  $z_f$ from 100-150 cm under the with-fallow rotation (Fig. 7B and D). This pattern is even stronger during the without-fallow rotation, such that thinner soils lose 16 times more water and nitrate than thicker soils, a more punctuated difference due to very low loss rates from the thickest soils with crop present. These findings of disproportionately high deep percolation rates through thinner soils agree with our prediction that thicker  $z_f$  soils mediate losses of water and nitrate to groundwater.

# 4.3. Fallow expands hot moments and hot spots

The relatively high rates of deep percolation simulated during fallow periods, along with observed accumulation of nitrate from mineralization in soils during fallow, provides support for our hypothesis that fallow primes soils for loss of water and nitrate. The propensity of the Crop-Fallow sequence to generate more deep percolation than the Fallow-Crop or Crop-Crop sequences was apparent across  $z_f$  values and was exemplified during high precipitation periods in 2011 and 2014 (Sup Materials 3.4). In addition to higher deep percolation, the warm and moist conditions during fallow periods facilitate mineralization of soil organic N to nitrate (Fig. 4; Vigil and Kissel, 1995; John et al., 2017; Sup Section 4.3), resulting in high leaching rates during the intense precipitation period (May-June) the following year. We observed the highest nitrate concentrations in lysimeters during Fallow-Crop years (Table 1), suggesting biogeochemical nitrate priming of soils in fallow years augments the fertilizer applied during the subsequent year to promote nitrate loss. This priming due to mineralization suggests that the duration of fallow influence extends beyond one third of the crop rotation. We observed an average of 34 kg ha<sup>-1</sup> of nitrate-N accumulated from mineralization approximately half-way through the fallow period (difference between profiles in Fig. 4B). This rate of nitrate accumulation aligns with modeled mineralization rates ranging from  $61\,$ to 77 kg ha<sup>-1</sup> yr<sup>-1</sup> for the full fallow period, reported by John et al. (2017), which equate to 70-90 % of N rates applied as fertilizer by our farmer-collaborators (83 to 91 kg ha<sup>-1</sup> yr<sup>-1</sup>).

Simulations also suggest that fallow practices increase the spatial extent of high deep percolation rates (i.e. expand hot spots). The  $z_f$  value for a given deep percolation rate was always higher for Crop-Fallow than

for the Fallow-Crop or Crop-Crop sequences (Fig. 7A). In the case of Field C, the simulated increase in spatial extent of hydrologically primed soils during fallow results in a disproportionately high fraction of overall deep percolation occurring during the Crop-Fallow sequence (55 %) relative to the cropped sequences (23–24 %; Sup Fig. 3.6a, panel C versus A & E).

#### 4.4. Management implications

The thickest soils and the rotation without fallow produce the highest transpiration and the lowest nitrate leaching rates. The general relationship between transpiration and crop yield (Musick et al., 1994; Rockstrom, 2003) suggests that crop-rotation and soil architecture scenarios that produce the highest transpiration rates may also produce the highest precipitation use efficiency; Hatfield et al., 2001). The precipitation use efficiency to transpiration correlation is complicated by non-linear reductions in yield depending on timing of water stress (Lehane and Staple, 1962; Campbell et al., 1977; Gu et al., 2020). Nonetheless, our model results highlight soil architecture  $(z_f)$  and rotation-related management opportunities to reduce nitrate leaching and increase precipitation use efficiency, simultaneously protecting groundwater quality and enhancing economic sustainability of agricultural operations. Reducing fallow periods and transitioning to continuous cropping or perennial vegetation on the thinnest  $z_f$  soils show the most promise for reducing nitrate leaching losses. These results also suggest that precision agriculture approaches that align seeding rates and fertilizer N application with spatially variable transpiration potential (a surrogate for yield potential) could reduce nitrate leaching. While the soils for the study area are abnormally thin on the spectrum of cultivated soils, simulations for thicker (>100 cm)  $z_f$  scenarios may approximate patterns expected for thicker soils in similar semi-arid locations. In addition, sensitivity analysis results for different soil textures and alternate values for other input parameters may facilitate extrapolation of results to additional scenarios. This type of broadly applicable tool for identifying control points may become increasingly important for sustainable agriculture, given climate projections for warmer temperatures and more intense precipitation events (Whitlock et al., 2017), which are likely to exacerbate hot moments of water and N use inefficiency.

#### 4.5. Emergent landscape-scale behavior

We assess the concept that whole-system water and N flux behavior can be predicted with a shifting mosaic of fallow land use overprinted on soil and precipitation derived control points, by comparing simulation results with emergent landscape scale patterns in deep percolation and nitrate leaching presented by Sigler et al. (2018). Deep percolation estimates by Sigler et al. (2018) were 8.7 cm yr<sup>-1</sup> for the Porter catchment (thin soils) and 5.4 cm  $yr^{-1}$  for the Kolin catchment (thick soils; Fig. 1), values bracketed by our model results applied with relevant  $z_f$  distributions and time periods (Table 4; Sup Section 4.5). The Sigler et al. (2018) estimates were based on stream flow measurements over the 2012-14 period, with estimates that groundwater-fed stream flows may lag behind precipitation patterns by up to one year. This suggests that the relevant period for comparison to modeling work here begins sometime in 2011 and runs through 2014. Exceptionally high precipitation in 2011 produced notably higher simulated deep percolation rates when that year was included (Table 4). The Sigler et al. (2018) deep percolation estimate for the Porter catchment (8.7 cm yr<sup>-1</sup>) falls between the 2011–2014 and the 2012–14 estimates from this work for  $z_f$ distributions based on both the Judith soil series  $(5.0-9.2 \text{ cm yr}^{-1})$  and the median of Field B soil pits (6.7–10.8 cm yr<sup>-1</sup>). Similarly, the Sigler et al. (2018) deep percolation estimate for the Kolin catchment (5.4 cm vr<sup>-1</sup>) falls between the 2011–2014 and the 2012–14 estimates from this work for  $z_f$  distributions based on both the Danvers soil series (2.0–5.7 cm  $yr^{-1}$ ) and the median of Field C soil pits (3.0–7.1 cm  $yr^{-1}$ ). This

agreement between our simulation results and an independent large-scale assessment of deep percolation lends credence to the idea that predictions of control points of episodic behavior may lead to reasonable estimates of landscape-scale phenomena.

Nitrate leaching rates estimated here from deep percolation weighted by  $z_f(2.2-13.8 \text{ kg N ha}^{-1} \text{ yr}^{-1}; \text{ Table 4})$  were somewhat lower than those from Sigler et al. (2018) at the catchment scale (11.1 kg ha<sup>-1</sup> yr<sup>-1</sup> Kolin; 18.4 kg ha<sup>-1</sup> yr<sup>-1</sup> Porter). The fact that simulated deep percolation rates align with previous work while nitrate leaching rates are low relative to previous work, points to characterization of N concentration in leachate as an imporant avenue for future work. Mean nitrate concentrations observed in lysimeters for all three 2-yr sequences were lower than the mean nitrate concentration in groundwater, suggesting that the higher nitrate concentrations observed in lysimeters during the Fallow-Crop sequence may be more representative of concentrations reaching groundwater. A fraction of N loss from soils may have also occurred as reduced N species not quantified in our lysimeter samples (ammonium or dissolved organic nitrogen). Reduced N species in leachate could be oxidized in the vadoze zone, augmenting the nitrate load reaching groundwater (Lorite-Herrera et al., 2009). In addition to enhanced biogeochemical analysis and modeling, future work incorporating snowmelt and the role of macropores as controls on deep percolation may increase model predictive power.

#### 5. Conclusions

Our results combine field observations with modeling to capture key interactions among crop rotation, soil architecture, and weather in cropping systems of the northern Great Plains that incorporate fallow. This synthesis highlights opportunities to increase water and N use efficiency for enhanced sustainability of agricultural yields in these systems that can also contribute to protection of environmental quality. In northern Great Plains agroecosystems, increased soil water storage during fallow periods facilitates mineralization of soil organic N to nitrate, resulting in elevated soil water and nitrate pools until the following growing season. Simulations suggest that fallow years account for 55 % of deep percolation and 43 % of leaching, despite fallow years only representing 33 % of the rotation. In this work, soils with  $z_f$  values thinner than 25 cm have mean precipitation storage efficiency values of zero and confer no water storage benefits to the crop following fallow, while facilitating nitrate leaching rates five to 16 times higher than thicker soils ( $z_f > 100$  cm). While there can be motivations for including fallow in rotation other than water storage, these areas with the lowest  $z_f$ values may be attractive candidates for conversion to perennial forage production or for annual cropping with lower N application rates. Future work to improve resolution and accuracy of mapped soil water holding capacity could be combined with this work to identify soils that produce low transpiration and economic returns while producing high leaching rates. These land areas with thin soil could be a focal point of programs incentivizing conversion to perennial vegetation or continuous cropping, with a likely outcome of reduced nitrate leaching and improved economic returns for farmers.

#### **Declaration of Competing Interest**

The authors report no declarations of interest.

#### Acknowledgements

The authors would like to thank cooperating farmers, local partners, and the MSU Central Agricultural Research Center (CARC). Thank you to field technicians Kyle Mehrens, Robby Robertson, Mike Bestwick, Joe Capella and a special thank you to Simon Fordyce who was the lead field technician for the majority of the field campaign. Venice Bayrd provided meticulous assistance with data curation and archiving. This work was funded by the United States Department of Agriculture, National

Institute of Food and Agriculture [grant number 2011-51130-31121, 2011] and USDA NIFA grant number 2016-67026-25067. Additional funding was provided by MSU Extension, Montana Fertilizer Advisory Committee, the Montana Agricultural Experiment Station and the Montana Institute on Ecosystems. This material is based upon work supported in part by the Consortium for Research on Environmental Water Systems (CREWS) National Science Foundation EPSCoR Cooperative AgreementOIA-1757351, as well as NSF EPSCoR Track 1 award numbers OIA-1443108 and EPS-1101342.

#### Appendix A. Supplementary data

Supplementary material related to this article can be found, in the online version, at doi:https://doi.org/10.1016/j.agee.2020.107158.

#### References

- Anapalli, S.S., Nielsen, D.C., Ma, L.W., Ahuja, L.R., Vigil, M.F., Halvorson, A.D., 2005. Effectiveness of RZWQM for simulating alternative great plains cropping systems. Agron. J. 97, 1183–1193. https://doi.org/10.2134/agronj2005.0019.
- Anderson, R.L., Bowman, R.A., Nielsen, D.C., Vigil, M.F., Aiken, R.M., Benjamin, J.G., 1999. Alternative crop rotations for the central Great Plains. J. Prod. Agric. 12, 95–99. https://doi.org/10.2134/jpa1999.0095.
- Bauder, J.W., Sinclair, K.N., Lund, R.E., 1993. Physiographic and land-use characteristics associated with nitrate-nitrogen in Montana groundwater. J. Environ. Qual. 22, 255–262.
- Bernhardt, E.S., Blaszczak, J.R., Ficken, C.D., Fork, M.L., Kaiser, K.E., Seybold, E.C., 2017. Control points in ecosystems: moving beyond the hot spot hot moment concept. Ecosystems 20, 665–682. https://doi.org/10.1007/s10021-016-0103-y.
- Bormann, F., Likens, G., 1979. Catastrophic disturbance and the steady-state in northern hardwood forests. Am. Sci. 67, 660–669.
- Burgess, M.H., Miller, P.R., Jones, C.A., 2012. Pulse crops improve energy intensity and productivity of cereal production in Montana, USA. J. Sustain. Agric. 36, 699–718. https://doi.org/10.1080/10440046.2012.672380.
- Campbell, C., Cameron, D., Nicholaichuk, W., Davidson, H., 1977. Effects of fertilizer-N and soil-moisture on growth, N-content, and moisture use by spring wheat. Can. J. Soil Sci. 57, 289–310. https://doi.org/10.4141/cjss77-035.
- Campbell, C.A., Selles, F., Zentner, R.P., De Jong, R., Lemke, R., Hamel, C., 2006. Nitrate leaching in the semiarid prairie: effect of cropping frequency, crop type, and fertilizer after 37 years. Can. J. Soil Sci. 86, 701–710.
- Cassman, K.G., Dobermann, A., Walters, D.T., Yang, H., 2003. Meeting cereal demand while protecting natural resources and improving environmental quality. Annu. Rev. Environ. Resour. 28, 315–358. https://doi.org/10.1146/annurev. energy.28.040202.122858.
- Di, H.J., Cameron, K.C., 2002. Nitrate leaching in temperate agroecosystems: sources, factors and mitigating strategies. Nutr. Cycl. Agroecosyst. 64, 237–256. https://doi.org/10.1023/A:1021471531188.
- Dockter, D., Palmer, P., 2008. Computation of the 1982 Kimberly-penman and the Jensen-Haise Evapotranspiration Equations As Applied in the U.S. Bureau of Reclamation's Pacific Northwest AgriMet Program. US Bureau of Reclamation.
- Farahani, H.J., Peterson, G.A., Westfall, D.G., 1998. Dryland cropping intensification: a fundamental solution to efficient use of precipitation. Adv. Agron. 64 (64), 197–223. https://doi.org/10.1016/S0065-2113(08)60505-2.
- Flury, M., Fluhler, H., Jury, W., Leuenberger, J., 1994. Susceptibility of soils to preferential flow of water - a field-study. Water Resour. Res. 30, 1945–1954. https://doi.org/10.1029/94WR00871.
- Foley, J.A., Ramankutty, N., Brauman, K.A., Cassidy, E.S., Gerber, J.S., Johnston, M., Mueller, N.D., O'Connell, C., Ray, D.K., West, P.C., Balzer, C., Bennett, E.M., Carpenter, S.R., Hill, J., Monfreda, C., Polasky, S., Rockstrom, J., Sheehan, J., Siebert, S., Tilman, D., Zaks, D.P.M., 2011. Solutions for a cultivated planet. Nature 478, 337–342. https://doi.org/10.1038/nature10452.
- Goulding, K., 2000. Nitrate leaching from arable and horticultural land. Soil Use Manage.
- Gu, Z., Qi, Z., Burghate, R., Yuan, S., Jiao, X., Xu, J., 2020. Irrigation scheduling approaches and applications: a review. J. Irrig. Drain. Eng. 146, 04020007 https:// doi.org/10.1061/(ASCE)IR.1943-4774.0001464.
- Hatfield, J.L., Sauer, T.J., Prueger, J.H., 2001. Managing soils to achieve greater water use efficiency: a review. Agron. J. 93, 271–280. https://doi.org/10.2134/ agroni2001.932271x.
- Huang, J., Ji, M., Xie, Y., Wang, S., He, Y., Ran, J., 2016. Global semi-arid climate change over last 60 years. Clim. Dyn. 46, 1131–1150. https://doi.org/10.1007/s00382-015-2636-8.
- John, A.A., Jones, C.A., Ewing, S.A., Sigler, W.A., Bekkerman, A., Miller, P.R., 2017.
  Fallow replacement and alternative nitrogen management for reducing nitrate leaching in a semiarid region. Nutr. Cycl. Agroecosyst. 108, 279–296. https://doi.org/10.1007/s10705-017-9855-9.
- Lanning, S.P., Kephart, K., Carlson, G.R., Eckhoff, J.E., Stougaard, R.N., Wichman, D.M., Martin, J.M., Talbert, L.E., 2010. Climatic change and agronomic performance of hard red spring wheat from 1950 to 2007. Crop Sci. 50, 835–841. https://doi.org/ 10.2135/cropsci2009.06.0314.

- Lawrence, P.G., Maxwell, B.D., Rew, L.J., Ellis, C., Bekkerman, A., 2018. Vulnerability of dryland agricultural regimes to economic and climatic change. Ecol. Soc. 23, 34. https://doi.org/10.5751/ES-09983-230134.
- Lehane, J.J., Staple, W.J., 1962. Effects of soil moisture tensions on growth of wheat. Can. J. Soil Sci. 42, 180–188. https://doi.org/10.4141/cjss62-023.
- Lorite-Herrera, M., Hiscock, K., Jimenez-Espinosa, R., 2009. Distribution of dissolved inorganic and organic nitrogen in river water and groundwater in an agriculturallydominated catchment, South-East Spain. Water Air Soil Pollut. 198, 335–346. https://doi.org/10.1007/s11270-008-9849-y.
- McClain, M.E., Boyer, E.W., Dent, C.L., Gergel, S.E., Grimm, N.B., Groffman, P.M., Hart, S.C., Harvey, J.W., Johnston, C.A., Mayorga, E., McDowell, W.H., Pinay, G., 2003. Biogeochemical hot spots and hot moments at the interface of terrestrial and aquatic ecosystems. Ecosystems 6, 301–312. https://doi.org/10.1007/s10021-003-0161-9.
- Miller, P.R., Bekkerman, A., Jones, C.A., Burgess, M.H., Holmes, J.A., Engel, R.E., 2015.
  Pea in rotation with wheat reduced uncertainty of economic returns in Southwest Montana. Agron. J. 107, 541–550. https://doi.org/10.2134/agroni14.0185.
- Mualem, Y., 1976. New model for predicting hydraulic conductivity of unsaturated porous-media. Water Resour. Res. 12, 513–522. https://doi.org/10.1029/ WR012i003p00513.
- Musick, J., Jones, O., Stewart, B., Dusek, D., 1994. Water-yield relationships for irrigated and dryland wheat in the Us Southern Plains. Agron. J. 86, 980–986. https://doi. org/10.2134/agronj1994.00021962008600060010x.
- Nielsen, D.C., Vigil, M.F., 2017. Intensifying a semi-arid dryland crop rotation by replacing fallow with pea. Agric. Water Manage. 186, 127–138. https://doi.org/ 10.1016/j.agwat.2017.03.003.
- Nielsen, D.C., Vigil, M.F., Anderson, R.L., Bowman, R.A., Benjamin, J.G., Halvorson, A. D., 2002. Cropping system influence on planting water content and yield of winter wheat. Agron. J. 94, 962–967. https://doi.org/10.2134/agronj2002.0962.
- Nielsen, D.C., Unger, P.W., Miller, P.R., 2005. Efficient water use in dryland cropping systems in the Great Plains. Agron. J. 97, 364–372. https://doi.org/10.2134/ agroni2005.0364.
- Or, D., Lehmann, P., Shahraeeni, E., Shokri, N., 2013. Advances in soil evaporation physics-a review. Vadose Zone J. 12 https://doi.org/10.2136/vzj2012.0163.
- Peterson, G.A., Schlegel, A.J., Tanaka, D.L., Jones, O.R., 1996. Precipitation use efficiency as affected by cropping and tillage systems. J. Prod. Agric. 9, 180–186.
- Ramankutty, N., Evan, A.T., Monfreda, C., Foley, J.A., 2008. Farming the planet: 1. Geographic distribution of global agricultural lands in the year 2000. Glob. Biogeochem. Cycles 22. https://doi.org/10.1029/2007GB002952. GB1003.
- Rockstrom, J., 2003. Water for food and nature in drought-prone tropics: vapour shift in rain-fed agriculture. Philos. Trans. R. Soc. Lond. Ser. B-Biol. Sci. 358, 1997–2009. https://doi.org/10.1098/rstb.2003.1400.
- Rockstrom, J., Falkenmark, M., 2000. Semiarid crop production from a hydrological perspective: gap between potential and actual yields. Crit. Rev. Plant Sci. 19, 319–346. https://doi.org/10.1016/S0735-2689(00)80007-6.
- Safriel, U., Adeel, Z., 2005. Dryland systems. In: Hassan, R., Scholes, R., Ash, N. (Eds.), Ecosystems and Human Well-Being: Current State and Trends Volume 1. Island Press Washington DC.
- Saseendran, S.A., Nielsen, D.C., Ma, L., Ahuja, L.R., Vigil, M.F., 2010. Simulating alternative dryland rotational cropping systems in the Central Great Plains with RZWQM2. Agron. J. 102, 1521–1534. https://doi.org/10.2134/agronj2010.0141.
- Schmidt, C., Mulder, R., 2010. Groundwater and Surface Water Monitoring for Pesticides and Nitrate in the Judith River Basin, Central Montana.
- Siebert, S., Doll, P., Hoogeveen, J., Faures, J.M., Frenken, K., Feick, S., 2005. Development and validation of the global map of irrigation areas. Hydrol. Earth Syst. Sci. Discuss. 9, 535–547. https://doi.org/10.5194/hess-9-535-2005.

- Siebert, S., Portmann, F.T., Döll, P., Siebert, S., Portmann, F.T., Döll, P., 2010. Global patterns of cropland use intensity. Remote Sens. 2, 1625–1643. https://doi.org/
- Sigler, W.A., Ewing, S.A., Jones, C.A., Payn, R.A., Brookshire, E.N.J., Klassen, J.K., Jackson-Smith, D., Weissmann, G.S., 2018. Connections among soil, ground, and surface water chemistries characterize nitrogen loss from an agricultural landscape in the upper Missouri River Basin. J. Hydrol. 556, 247–261. https://doi.org/ 10.1016/j.jhydrol.2017.10.018.
- Sigler, W.A., Ewing, S.A., Payn, R.A., Jones, C.A., 2020. Cultivated soil water dynamics with many Hydrus 1D simulations using R. HydroShare. https://doi.org/10.4211/ hs.fd6cd94345f9420f97d63753fc850c41.
- Simunek, J., Sejna, M., Saito, H., van Genuchten, M.Th, 2013. HYDRUS-1D Software Package for Simulating the Movement of Water, Heat, and Multiple Solutes in Variably Saturated Media. Version 4.16, HYDRUS Software Series 3, 2013. Department of Environmental Sciences, University of California Riverside, Riverside, California, USA, p. 340.
- Šimůnek, J., Šejna, M., van Genuchten, M.T., 2020. Hydrus 1D archive of version 4.16.0110, replicated from: Simůnek, J., M. Šejna, and M. Th. van Genuchten. 2019. Hydrus-1D for Windows, Version 4.xx. https://www.pc-progress.com/en/Default. aspx?hydrus-1d, accessed 7/23/2020, replicated in HydroShare at:. https://doi.org/ 10.4211/hs.d24921ba081d431e80685bf177a0840f40f.
- Smith, V.H., 2003. Eutrophication of freshwater and coastal marine ecosystems a global problem. Environ. Sci. Pollut. Res. 10, 126–139. https://doi.org/10.1065/ espr2002.12.142.
- Spalding, R.F., Exner, M.E., 1993. Occurrence of nitrate in groundwater—a review. J. Environ. Qual. 22, 392–402. https://doi.org/10.2134/ jeq1993.00472425002200030002x.
- Tesoriero, A.J., Duff, J.H., Saad, D.A., Spahr, N.E., Wolock, D.M., 2013. Vulnerability of streams to legacy nitrate sources. Environ. Sci. Technol. 47, 3623–3629. https://doi. org/10.1021/es305026x.
- Thorup-Kristensen, K., Cortasa, M.S., Loges, R., 2009. Winter wheat roots grow twice as deep as spring wheat roots, is this important for N uptake and N leaching losses? Plant Soil 322, 101–114.
- Twarakavi, N.K.C., Sakai, M., Simunek, J., 2009. An objective analysis of the dynamic nature of field capacity. Water Resour. Res. 45, W10410 https://doi.org/10.1029/ 2000WB007944
- Vick, E.S.K., Stoy, P.C., Tang, A.C.I., Gerken, T., 2016. The surface-atmosphere exchange of carbon dioxide, water, and sensible heat across a dryland wheat-fallow rotation. Agric. Ecosyst. Environ. 223, 129–140. https://doi.org/10.1016/j. agee.2016.07.018.
- Vigil, M., Kissel, D., 1995. Rate of nitrogen mineralized from incorporated crop residues as influenced by temperature. Soil Sci. Soc. Am. J. 59, 1636–1644.
- Wang, T., Istanbulluoglu, E., Lenters, J., Scott, D., 2009. On the role of groundwater and soil texture in the regional water balance: an investigation of the Nebraska Sand Hills, USA. Water Resour. Res. 45, W10413 https://doi.org/10.1029/ 2009WR007733.
- Ward, M.H., deKok, T.M., Levallois, P., Brender, J., Gulis, G., Nolan, B.T., VanDerslice, J., International Society for Environmental Epidemiology, 2005. Workgroup report: drinking-water nitrate and health–recent findings and research needs. Environ. Health Perspect. 113, 1607–1614.
- Whitlock, C., Cross, W., Maxwell, B., Silverman, N., Wade, A.A., 2017. 2017 Montana Climate Assessment. Montana State University and University of Montana, Montana Institute on Ecosystems, Bozeman and Missoula MT. https://doi.org/10.15788/ m2ww8w.